Strong enhancement of direct transition photoluminescence with highly tensile-strained Ge grown by molecular beam epitaxy

Yijie Huo, ^{1,a)} Hai Lin, ² Robert Chen, ^{1,b)} Maria Makarova, ¹ Yiwen Rong, ¹ Mingyang Li, ³ Theodore I. Kamins, ¹ Jelena Vuckovic, ¹ and James S. Harris

(Received 30 June 2010; accepted 13 December 2010; published online 6 January 2011)

Highly tensile-strained layers of Ge were grown via molecular beam epitaxy using step-graded $In_xGa_{1-x}As$ buffer layers on (100) GaAs. These layers have biaxial tensile-strain of up to 2.33%, have surface roughness of <1.1 nm, and are of high quality as seen with transmission electron microscopy. Low-temperature photoluminescence (PL) suggests the existence of direct-bandgap Ge when the strain is greater than 1.7%, and we see a greater than $100\times$ increase in the PL intensity of the direct transition with 2.33% tensile-strain over the unstrained case. These results show promise for the use of tensile-strained Ge in optoelectronics monolithically integrated on Si. © 2011 American Institute of Physics. [doi:10.1063/1.3534785]

The path to integrated optoelectronics on Si has made much progress in recent years through the investigation of tensile-strained Ge. Ge has been theoretically predicted to become direct-bandgap with about 1.7% biaxial tensile-strain due to the Γ band-edge decreasing more rapidly than the L band-edge with increased tensile-strain. This has generated much interest because a direct-bandgap material that is compatible with Si has the potential to create optoelectronic devices integrated on Si, which provides both a cost advantage and applications for optical interconnects on-chip. Furthermore, direct-bandgap Ge can be used as the gain medium for a group-IV laser, considered to be the "holy-grail" of Si photonics.

Despite the advantages and promise of tensile-strained Ge, the amount of strain needed for the direct-bandgap transition is difficult to achieve due to the need for coherent Ge growth on a material with an adequately large lattice constant. Still, much work has been done to achieve high strain or direct-bandgap properties, including the use of relaxed In_xGa_{1-x}As buffer layers^{3,4} to achieve up to 1.55% tensilestrained Ge and the use of the thermal expansion coefficient difference between Si and Ge to grow tensile-strained Ge directly on Si to achieve 0.3% tensile-strain. However, both these methods did not show evidence of direct-bandgap Ge, most likely due to sub-1.7% strain percentage. Although this strain is not sufficient for direct-bandgap Ge, Sun⁶ and Cheng both used this technique in conjunction with high n-doping to fill the L valley, thus shifting the Fermi level closer to the Γ valley and increasing the carrier population in that valley. Through this technique, they have both demonstrated electroluminescence in light-emitting diode devices fabricated with these strained structures. Furthermore, Liu et al.8 recently demonstrated an optically pumped Ge laser using strain and n-doping. However, their efficiencies are very low, possibly due to free-carrier absorption. A directbandgap material without significant doping is not expected to suffer from these issues. In this letter, we report the

All of our samples were grown on (100) semi-insulating GaAs wafers. We used a modified Varian Gen II III-V molecular beam epitaxy (MBE) system for In_xGa_{1-x}As buffer layer growth. First, a 100 nm buffer layer of GaAs was grown on the wafer to improve the surface quality. In situ reflection high energy electron diffraction (RHEED) was used to verify the quality of the surface prior to further growth. Next, step-graded In_xGa_{1-x}As buffer layers were grown to increase the lattice constant at the top of the structure. Substrate growth temperatures for the buffer layers were all below 400 °C thermocouple (TC) reading. To ensure the relaxation of the buffer layers, the thickness of each layer is 200 nm, which is greater than the critical thickness for the layers. Threading dislocations due to relaxation were terminated using high-temperature in situ anneals of 520-540 °C TC between each buffer layer. The samples were then transferred under ultrahigh vacuum (10^{-9} torr) to a group-IV MBE chamber for Ge growth. In this chamber, a 10 nm thick Ge layer without intentional doping was coherently grown at a rate of 1 nm per min at TC 400 °C. To ensure high quality planar growth, in situ RHEED was used to verify the 2×4 pattern for $In_rGa_{1-r}As$ and 2×1 pattern for Ge. Finally, an In_rGa_{1-r}As cap layer was grown for sur-

TABLE I. Strain calculated from theory, XRD, and Raman spectroscopy, and the corresponding AFM RMS roughness.

Indium (%)	Theory (%)	Raman (%)	XRD (%)	AFM RMS (nm)
10	0.64	0.26	0.42	0.20
20	1.35	0.91	0.93	0.67
30	2.07	1.78	1.84	0.51
40	2.79	2.35	2.31	1.01

¹Electrical Engineering, Stanford University, Stanford, California 94305, USA

²Materials Science and Engineering, Stanford University, Stanford, California 94305, USA

³Department of Physics, Stanford University, Stanford, California 94305, USA

growth and characterization of thin Ge layers that are highly tensile strained (up to 2.33%) using $In_xGa_{1-x}As$ buffer layers with high In concentration of up to x=0.40. These structures have the highest amount of tensile-strain reported in Ge. These samples also exhibit excellent luminescent properties, thereby suggesting direct-bandgap behavior.

^{a)}Electronic mail: yjhuo@stanford.edu.

b) Electronic mail: robert.chen@stanford.edu.

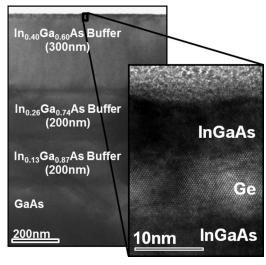


FIG. 1. TEM image of 2.3% tensile-strained Ge on $\rm In_{0.40} Ga_{0.60} As$. The buffer layer and the 10 nm Ge layer are smooth and free from visible dislocations. The high-resolution image on the right shows fault-free stacking of Ge atoms.

face passivation to prevent Ge oxidation, eliminate surface states, and improve carrier confinement during optical characterization.

Material characterization to investigate material quality and strain was conducted using atomic force microscopy (AFM) (Park System XE-70), transmission electron microscopy (TEM) (Philips CM20 FEG-TEM), x-ray diffraction (XRD) (PANalytical X'Pert PRO), and Raman spectroscopy (Renishaw RM Series System 1000 with a 50 mW Ar⁺ laser at 514 nm). Noncontact mode AFM was used to characterize the sample surface morphology. The root means square (rms) surface roughness for a $1 \times 1 \mu m^2$ region for various samples is listed in Table I. The rms roughness for our samples is very low, ranging from 0.20 nm for x=0.10 and 1.01 nm for x=0.40. This suggests a smooth buffer layer and epitaxial Ge growth. The cross-section TEM images of 2.33% tensile-strained Ge on $In_{0.40}Ga_{0.60}As$ confirm these results and are shown in Fig. 1. Planar growth is clearly seen for the Ge layer, and the perfect lattice fringes of Ge can be seen in the high-resolution TEM (HR-TEM) image. No dislocations are observed in the Ge region of the HR-TEM, indicating dislocation densities in the 10⁷ cm⁻² regime.

The composition and strain of In_xGa_{1-x}As buffer layers were characterized by XRD reciprocal space mapping at (004) and (224) Bragg reflections. Figure 2 shows the (004) and (224) reciprocal space maps (RSMs) for a sample with three step-graded In_xGa_{1-x}As buffer layers on a GaAs substrate. The tilting for the three buffer layers is negligible. We should note that the thin 10 nm Ge layer is not visible in this map because its signal is below the noise level. As the figure shows, the buffer layers are very close to the relaxation line, thereby suggesting high relaxation in these layers. Numerical analysis indicates relaxation percentages of greater than 89% for all layers. From the XRD RSM, the lattice constant is calculated to be 5.792 Å for the top $In_{0.40}Ga_{0.60}As$. With the coherent growth of Ge suggested earlier, we determine that the strain in the Ge layer is around 2.37%. Some slight error (<0.1% in the strain) may exist due to the uncertainty in determining the center of the reciprocal peak and the chance of partial relaxation of the Ge layer under high tensile-strain. The strain percentages of the Ge layer grown on various

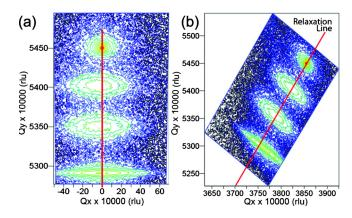


FIG. 2. (Color online) X-ray diffraction 2D reciprocal space mapping at (a) (004) and (b) (224) for Ge on $In_{0.40}Ga_{0.60}As$. The relaxation line is shown to confirm our step-graded buffer layer approach.

 $In_xGa_{1-x}As$ layers calculated from XRD RSMs are shown in Table I.

Raman spectroscopy was also used to determine the strain percentage of the Ge layers. The Raman spectra were taken at room temperature in a (001) backscattering geometry. For this configuration, only the longitudinal optical phonon mode can be detected. As can be seen from Fig. 3, the Ge peak Raman shift for each sample indicates increasing tensile-strain from the bulk Ge reference. The amount of tensile-strain can be calculated from the Raman shift $(\Delta \omega)$ relative to the bulk Ge. The equation can be simplified to $\Delta \omega = b \epsilon_{\parallel}$, where ϵ_{\parallel} is the biaxial tensile-strain and $b = -(415 \pm 40)$ cm⁻¹ (Ref. 9). The smaller Raman peak in the spectrum corresponds to the $In_xGa_{1-x}As$ buffer layers. The amount of tensile-strain in the Ge calculated from Raman spectroscopy is also shown in Table I.

The strain percentages measured by Raman and determined through XRD are in agreement with each other, as shown in Table I. Additionally, these measured results are in good agreement with theory, which determines the strain assuming coherent growth of Ge on $In_xGa_{1-x}As$. The theoretical model assumes full relaxation of the $In_xGa_{1-x}As$ layer, which is why the strain determined from XRD and Raman is slightly less. Through analysis of the XRD and Raman measurements, we have determined that our Ge layer on $In_{0.40}Ga_{0.60}As$ is 2.33% tensile strained, which is the highest reported tensile-strain on Ge to date.

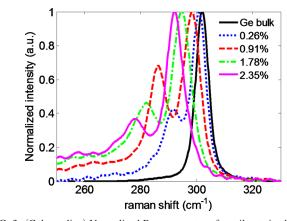


FIG. 3. (Color online) Normalized Raman spectra of tensile-strained Ge on various $In_xGa_{1-x}As$ buffer layers. The Raman shift is due to the amount of strain applied to the Ge layer. Bulk Ge is shown as a reference.

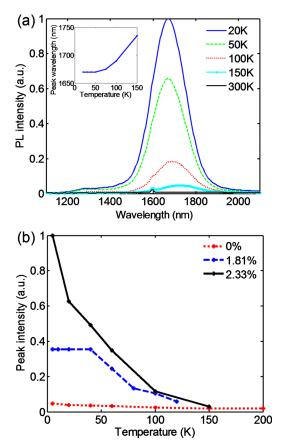


FIG. 4. (Color online) (a) Normalized PL intensity of the 2.33% tensile-strained Ge sample with $In_{0.40}Ga_{0.60}As$ buffer layers. The small peak around 1596 nm is due to the excitation laser line. The inset shows the change in peak wavelength with temperature. (b) Comparison of normalized (relative to each other) PL peak intensity for 2.33%, 1.81%, and unstrained Ge samples.

With a measured tensile-strain greater than the amount theoretically predicted to produce direct-bandgap Ge, we proceeded with photoluminescence (PL) measurements. The temperature-dependent PL spectrum of our 2.33% sample is shown in Fig. 4(a). The data show an intensity peak around 1670 nm at 20 K for the 2.33% sample. If we assume that the emission peak is centered at the bandgap, this corresponds to a transition energy of around 0.743 eV, which is higher than the predicted direct-bandgap at 2.33% strain. This discrepancy, however, is predicted by the authors of Ref. 2 since the theoretical bandstructure calculations were done using deformation potentials accurate only for small-strain conditions. Other factors, such as the increase in bandgap with decrease in temperature, increase in the ground-state energy due to quantum confinement with the In_rGa_{1-r}As barriers, and the possibility of an energy shift of the peak carrier concentration with high injection due to a shift in the quasi-Fermi level can also contribute to an increase in effective transition energy. The shoulders seen at wavelengths less than 1400 nm are due to the buffer layers since In_{0.4}Ga_{0.6}As at room temperature is expected to have a peak around 1386 nm. 10 Additionally, any decrease in either temperature or In concentration is expected to increase the bandgap (thus decreasing the emission wavelength).

In Fig. 4(b), we show the peak intensity for samples with different strain, including an unstrained sample of Ge grown directly on GaAs with a GaAs cap. We see that at 5 K the PL peak intensity for the 2.33% sample is more than $2.5 \times$ greater than the 1.81% sample and more than 20× greater than the unstrained sample under the same pumping and detection conditions. We should note that the peak with the greatest intensity is used for this comparison—in the unstrained case, the peak from the indirect transition, and in the 2.33% strain sample, the peak is from the direct transition. The signal from direct transition in the unstrained case is below the noise floor of our system, meaning that the direct transition enhancement is at least 100× that of the unstrained case. From this, we conclude that there is a strong enhancement in the PL peak intensity from the direct transition with increasing strain.

In summary, we have used MBE to grow up to 2.33% tensile-strained Ge on In_xGa_{1-x}As buffer layers, producing the highest reported strain percentage in Ge to date. Low growth temperatures and low growth rates enabled the 2D growth of coherent tensile-strained Ge. Material quality and strain were gauged using TEM, AFM, XRD, and Raman spectroscopy, and these measurements resulted in strain percentages that were in agreement with each other and matched theoretical predictions. Furthermore, optical characterization using low-temperature PL showed a strong increase in PL intensity with higher strain percentages, namely, for 1.81% and 2.33% tensile-strained Ge samples. This increase in PL intensity shows that direct-bandgap, tensile-strained Ge may be a strong candidate for a group-IV laser. With the ability to synthesize highly strained layers of Ge, we can further investigate optical and transport properties of a material that may have a place in future devices and optoelectronics on Si.

This work was carried out as part of the Interconnect Focus Center Research Program, supported by the Microelectronics Advanced Research Corporation (MARCO). We also acknowledge the Air Force Office of Scientific Research for their financial support under Contract No. FA9550-06-532.

 ¹R. A. Soref and L. Friedman, Superlattices Microstruct. 14, 189 (1993).
²M. V. Fischetti and S. E. Laux, J. Appl. Phys. 80, 2234 (1996).

³Yu. Bai, K. E. Lee, C. Cheng, M. L. Lee, and E. A. Fitzgerald, J. Appl. Phys. **104**, 084518 (2008).

⁴Y. Hoshina, A. Yamanda, and M. Konagai, Jpn. J. Appl. Phys. **48**, 111102 (2009).

⁵J. F. Liu, D. D. Canon, K. Wada, Y. Ishikawa, S. Jongthammanurak, D. T. Danielson, J. Michel, and L. C. Kimerling, Appl. Phys. Lett. **87**, 011110 (2005).

⁶X. Sun, J. Liu, L. C. Kimerling, and J. Michel, Opt. Lett. **34**, 1198 (2009). ⁷S.-L. Cheng, J. Lu, G. Shambat, H.-Y. Yu, K. Saraswat, J. Vuckovic, and Y. Saraswat, Opt. Express **17**, 10019 (2009).

⁸J. Liu, X. Sun, R. Camacho-Aguilera, L. C. Kimerling, and J. Michel, Opt. Lett. **35**, 679 (2010).

⁹Y. Y. Fang, J. Tolle, R. Roucka, A. V. G. Chizmeshya, J. Kouvetakis, R. R. D'Costa, and J. Menendez, Appl. Phys. Lett. **90**, 061915 (2007).

¹⁰R. E. Nahory, M. A. Pollack, W. D. Johnston, Jr., and R. L. Barns, Appl. Phys. Lett. **33**, 659 (1978).